

Inelastic Behavior of Thin-walled Circular Steel Tubular Columns Under Pushover and Cyclic Loading

Njiru Mwaura¹, Iraj H.P. Mamaghani¹

¹Department of Civil Engineering, University of North Dakota
243 Centennial Drive Stop 8115, Grand Forks, ND, USA
njiru.mwaura@und.edu; iraj.mamaghani@und.edu

Abstract - Thin-walled circular steel tubular columns have been used as bridge piers widely around the globe because of their excellent seismic performance: ductility, strength, and energy dissipation capacity. This paper investigates the inelastic behavior of thin-walled circular steel tubular columns with a uniform cross-section. The loading protocol considered for this study is either pushover or cyclic lateral loading in the presence of a constant axial load. The effects of a pushover and cyclic lateral loading on the behavior of the thin-walled circular steel tubular columns modeling bridge piers have been evaluated through analysis of failure mode, hysteresis curve, envelope curve, stiffness, and strength degradation characteristics, including pre-and post-buckling regimes. The study applies the finite element model (FEM) that considers the effect of both material and geometric nonlinearities. Also, in an accompanying paper, a comprehensive parametric study was carried out to investigate the effects of the critical design parameters and namely are: the radius to thickness parameter (R_t), the column slenderness ratio parameter (λ), and the magnitude of axial load (P/P_y). Finally, a series of proposed formulae for strength and ductility evaluation for thin-walled circular steel tubular columns are given.

Keywords: Thin-Walled, Steel, Tubular Columns, Ductility, Strength, Inelastic Behavior, Pushover, Cyclic Loading, Finite Element Analysis, Local Buckling

1. Introduction

Bridge piers and columns in buildings have predominantly been constructed of structural steel [1]. Thin-walled circular steel tubular columns modeling bridge piers, with and without longitudinal and lateral stiffeners, in the form of cantilever columns and planar rigid frames, have been used in modern highway bridge systems because of their high strength and torsional rigidity. For example, Figure 1 shows bridge piers of thin-walled circular and rectangular box sections supporting an elevated highway bridge in Nagoya, Japan [2]. These structures experience damage caused by local buckling, global buckling, or an interaction of both. Local buckling is characterized by a sizeable width-to-thickness ratio of the flange plate (for the box section) and a sizeable radius-to-thickness ratio of the circular section.

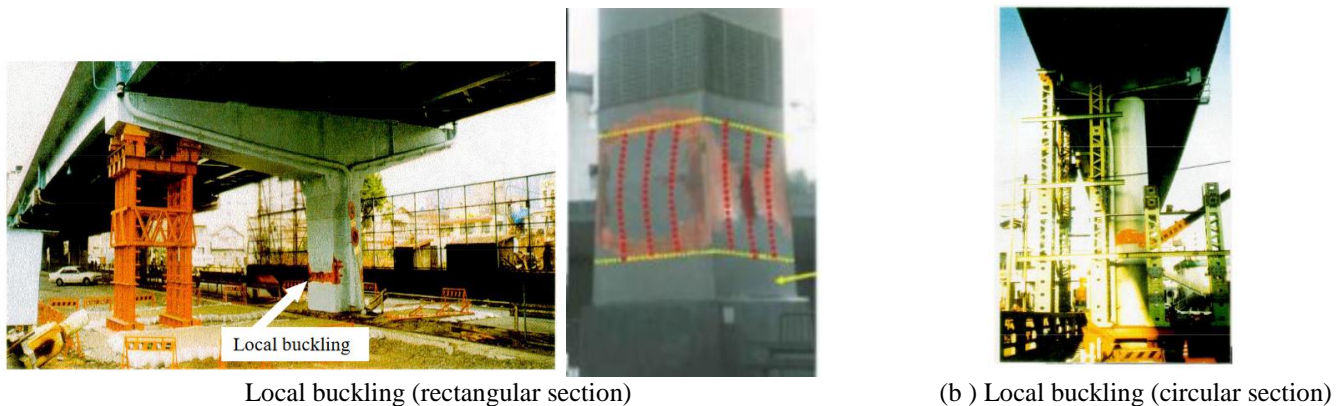


Fig. 1: Damaged bridge piers in the Kobe Earthquake, 1995 [2].

Figure 1 indicates the effects of the Kobe earthquakes on various bridges in Japan after the Kobe earthquake in 1995. The figure shows the occurrence of local buckling on bridge piers due to inelastic behavior and severe earthquake, as shown on the thin-walled tubular columns. The Kobe earthquake was assigned a magnitude of 7.2 by the Japan Meteorological Agency (JMA), and the epicenter was located approximately 20 km South-West of Kobe city [3]. It destroyed many elevated

roadways, and since then Kobe earthquake has inspired researchers to investigate the strength and ductility of thin-walled steel tubular columns and their impact on preventing the collapse of bridges during strong earthquakes.

Researchers have been conducting experiments and studies on applications of thin-walled steel tubular columns and their advantages in earthquake-prone areas [4-12]. Thin-walled steel tubular columns possess valuable benefits compared to conventional ones made of reinforced concrete. Thin-walled steel tubular columns are more efficient due to their lightweight, high strength, ductility, ease, and speed of construction, especially when limited construction space is needed [2].

Research, including experimental and numerical analyses, has been conducted to identify methods that improve the strength and ductile behavior of the thin-walled steel columns under constant axial force and cyclic lateral loading [13-24]. Observations on thin-walled steel tubular columns after major earthquakes have shown their vulnerability to local and global buckling [9].

Accurate numerical models are necessary to evaluate the seismic performance and loading bearing mechanism of thin-walled steel tubular columns [23]. This paper presents a numerical finite element analysis of thin-walled circular steel tubular columns regarding local buckling and their ultimate strength, ductility, energy absorption, and pre-and post-buckling behavior under a constant axial and pushover or cyclic lateral loading. The experiments conducted in Japan [16, 17] were used to substantiate the finite element modeling (using ABAQUS/Standard version 6.14 adopted in this study). The adopted FEM accounts for both material and geometrical nonlinearities.

2. Thin-Walled Circular Steel Tubular Columns

Thin-walled circular steel tubular columns with a fixed base, EM) accuracy as illustrated in Figure 2, have widely been used in Japan as piers for highway bridges [8, 11, 21]. The thin-walled circular steel tubular column modeling bridge piers are subjected to a constant axial force (P) and cyclic lateral load (H), as shown in Figure 2(a). The axial load is a vertical load applied at the centroid of the column cross-section. The axial load (P) accounts for service gravity loads (dead and live loads) that act on the column during its lifetime. In the presence of constant axial load, the cyclic horizontal lateral load is considered to stimulate seismic loads. The strength and ductility of thin-walled circular steel tubular column modeling bridge piers are investigated with pre-and post-buckling regimes. The lateral load is applied as a displacement at the top of the column. The post-buckling behavior that simulates maximum column deterioration is monitored depending on whether the loading protocol is a pushover or cyclic lateral loading. The pushover loading considers one large displacement applied monotonically up to $8\delta_y$, while the cyclic lateral load considers unidirectional loading cases where the lateral displacement is increased in multiples of yield displacement $m\delta_y$ ($m=1, 2, 3, \dots, 8$) in alternate directions, Figure 3.

The strength and ductility of thin-walled circular steel tubes are affected by the radius to thickness ratio parameter (R_t) of the cross-section and slenderness ratio (λ) of the columns [2, 4]. R_t controls the local buckling behavior of the plate, while λ has a considerable effect on the global stability of the column [4, 16]. For the thin-walled circular steel tubular columns, definitions of R_t and λ parameters are given as [4]:

$$R_t = \frac{D_o \sigma_y}{2t_s E_s} \sqrt{3(1 - \nu_s^2)} \quad (1)$$

$$\lambda = \frac{1}{\pi} \sqrt{\frac{\sigma_y 2h}{E_s r_s}} \quad (2)$$

Where, D_o = outer diameter (mm), t = wall thickness (mm), r_s = radius of gyration (mm), σ_y = yield stress (N/mm²), E_s = Young's modulus (N/mm²), ν_s = Poison's ratio, h = height of the column (mm).

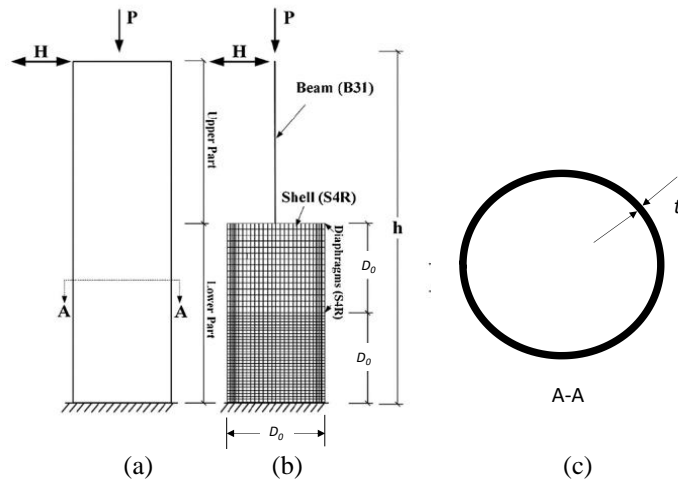


Fig. 2: Column model: (a) Column, (b) FE Meshing, (c) Cross-Section A-A.



Fig. 3: Cyclic loading path protocol.

2.1. Finite Element Modelling

Finite element analysis was conducted using commercial finite element software, Abaqus/Standard version 6.14 [25]. Finite element modeling considers first the choice of the geometric discretization shapes that are efficient and saves computation time. Thin-walled steel tubular columns are divided into segments, and each piece meshes in consideration for quick convergence of the solution. The lower segment, discretized using shell element, is divided into two lower and upper parts. It's lower part (with a height equivalent to the diameter of the tube, D_0) is finely meshed compared to the upper part. The upper segment is discretized as a beam element. In Abaqus documentation, the shell element denoted as SR4 uses a 4-node reduced integration shell element. In addition, it also utilizes five Gaussian integration points across its cross-section to distribute plasticity [25]. The beam element, denoted as B31, considers two nodes at every discretization region in one dimension, and its consideration makes computation faster due to its simplicity.

Figure 2(b) indicates the meshing sizes for height equivalent to D_0 and the entire column. The column was modeled as a shell element SR4 for the height equal to $2D_0$. A beam-column element (B31) was adopted for the upper part ($h-2D_0$). The S4R and B31 elements have been modeled using multi-point interface constraint (MPC). Analytical efficiency was improved by dividing the thin-walled circular steel tubular columns into sections; the lower part of the thin-walled circular steel column (equal to the diameter of the tube, D_0) meshed to S4R elements of size 20mm, and another D_0 on top of the lower part meshed to S4R elements of size 40mm. The upper segment of the column ($h-2D_0$) was considered a beam-column divided into B31 elements with a dimension of 100mm. The mesh sizes stated above were decided by trial and error, and the displacement convergence criterion for this analysis considered a convergence tolerance of 10^{-5} and 300 iterations. The initial geometrical imperfection and residual stresses were neglected for this analysis as previous studies indicated that they have a negligible effect on the cyclic behavior of analyzed columns [4].

2.2. Material Behavior

The inelastic behavior of thin-walled steel structures is dependent on the mechanical property observed in the stress-strain relationship. Pushover and cyclic lateral loading are modeled under different material models available in various FEM software. In this study, the multilinear kinematic hardening material model, Figure 4, is used in the analysis as it predicts material behavior better than the isotropic hardening material model [2, 13].

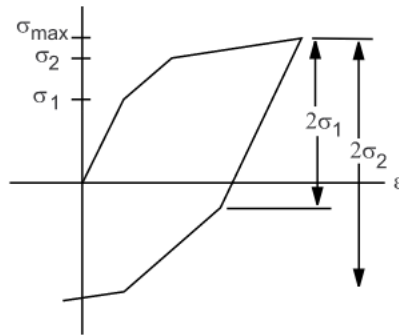


Fig. 4: Multi-linear kinematic [25].

2.3 Initial yield load and yield displacement

The initial yield displacement δ_y and the corresponding horizontal lateral load H_y are given by the following equations [2]:

$$\delta_y = \frac{H_y h^3}{E_s I_s} \quad (4)$$

$$H_y = \left(\sigma_y - \frac{P}{A_s} \right) \frac{S_s}{h} \quad (5)$$

Where, H_y , $E_s I_s$, A_s and S_s denote the lateral yield force, bending rigidity, cross-section area, and elastic section modulus, respectively, of a cantilevered hollow steel tube with a fixed base, Figure 1(a). The yield displacements and lateral yield loads for all analyzed columns are listed in Table 1.

Table 1: Geometric, Material properties, and initial displacement of the analyzed columns.

| Column | h (mm) | D_0 (mm) | t (mm) | P/P_y | σ_y (Mpa) | σ_u (Mpa) | E (GPa) | H_y (kN) | δ_y (mm) | R_t | λ |
|----------|-------------|---------------|-------------|---------|---------------------|---------------------|--------------|---------------|--------------------|-------|-----------|
| P5-e0 | 4391 | 891 | 8.4 | 0.150 | 235.0 | 426 | 206 | 232.0 | 14.0 | 0.10 | 0.30 |
| P1 | 3403 | 891 | 9.0 | 0.120 | 289.6 | 510 | 206 | 415.2 | 10.6 | 0.11 | 0.26 |
| C column | 3403 | 900 | 9.0 | 0.124 | 298.6 | 495 | 206 | 414.9 | 10.6 | 0.12 | 0.26 |

All columns are loaded with one-cycle at each displacement ($N = 1$), $P_y = \sigma_y \cdot A$, $A = \pi (D_0^2 - D_i^2)/4$, $D_i = D_0 - 2t$, t = thickness of plate for the column, $I = \pi (D_0^4 - D_i^4)/64$, $S = \text{elastic section modulus} = \pi (D_0^4 - D_i^4)/32D_0$, D_0 = Outer diameter of the tube, D_i = Inner diameter of the tube.

3. Comparison of Analysis and Test Results

This section presents the computed normalized lateral load versus lateral displacement hysteresis and envelope curves for the tested columns (P5-e0, P1, and C). The accuracy of the employed FEM has been substantiated using experimental results obtained from Japan [16, 17]. Table 2 lists strength and ductility results for the analyzed columns.

Table 2: Strength and ductility of the validated tubular columns.

| Column | | Strength and Ductility Ratio (Cyclic) | | | | Strength and Ductility Ratio (Pushover) | | | |
|--------|----------|--|---------------|---------------------|-------------------------|--|---------------|---------------------|-------------------------|
| | | H_{max}/H_y | $H_{0.9}/H_y$ | δ_m/δ_y | $\delta_{0.9}/\delta_y$ | H_{max}/H_y | $H_{0.9}/H_y$ | δ_m/δ_y | $\delta_{0.9}/\delta_y$ |
| P5-e0 | Analysis | 1.46 | 1.32 | 1.9 | 3.0 | 1.46 | 1.32 | 1.9 | 3.0 |
| | Test | 1.46 | 1.32 | 1.9 | 3.0 | 1.46 | 1.32 | 1.9 | 3.0 |
| P1 | Analysis | 1.45 | 1.31 | 2.4 | 2.9 | 1.45 | 1.31 | 2.4 | 3.0 |
| | Test | 1.45 | 1.31 | 2.4 | 2.9 | 1.41 | 1.27 | 2.4 | 2.9 |
| C | Analysis | 1.45 | 1.31 | 2.4 | 3.1 | 1.45 | 1.31 | 2.4 | 3.9 |
| | Test | 1.45 | 1.31 | 2.4 | 3.1 | 1.45 | 1.31 | 2.4 | 3.9 |

3.1. Pushover Behavior

These curves were developed by giving the columns one large displacement ($8\delta_y$). The experiment and the FE analysis exhibited a close agreement. Figure 5 compares the normalized lateral load versus lateral displacement curves of the columns (P5-e0 and C) obtained from the analysis and experiment under the pushover lateral displacement history. The solid line denotes numerical results, while the dashed line stands for the experimental results. H_y and δ_y represent the lateral yield load and the corresponding lateral yield displacement. As shown in Fig. 5, there is a good match between the experimental and analysis results, indicating the adopted finite element modeling and analysis accuracy.

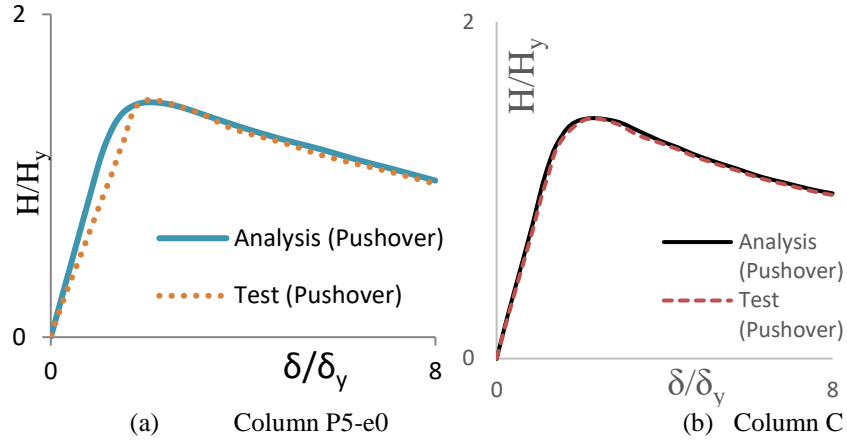


Fig. 5: Comparison of pushover curve from tests and analysis.

3.2. Hysteresis Behavior

Figure 6 compares the columns' normalized lateral load versus lateral displacement hysteresis curves (P5-e0 and P1). The solid line denotes numerical results, while the dashed line stands for the experimental results. As shown in Fig. 6, there is a good match between the experimental and analytical results under cyclic loading. Referring to Table 2, the FEM predicts the ultimate strength of the uniform thin-walled circular steel tubular columns with less than a 3% error. This indicates that FE analysis, using the assumed geometric and material model, captured the structural hysteresis behavior of thin-walled circular steel tubular columns under cyclic loading.

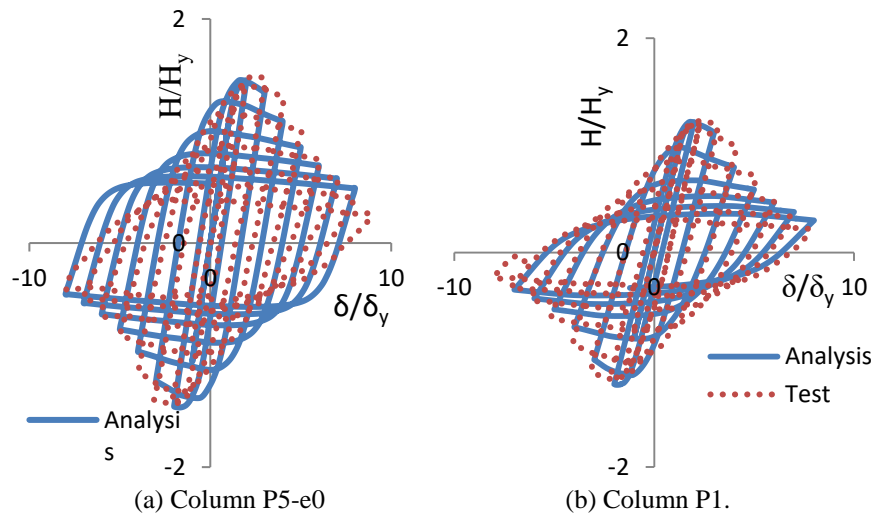


Fig. 6: Comparison of hysteresis behavior from tests and analysis.

3.3. Envelope Curves

The envelope curves were developed from the hysteresis loops above by determining the peak strengths on all whole number amplitudes. Figure 7 shows a close agreement of envelope curves for the test and the FE analysis.

4. Conclusion

The inelastic behavior of prismatic thin-walled circular steel tubular columns under pushover and cyclic lateral loading in the presence of constant axial load was investigated. The effects of a pushover and cyclic lateral loading on the behavior of the thin-walled circular steel tubular bridge piers have been evaluated through analysis of failure mode, hysteresis curve, envelope curve, stiffness, and strength degradation characteristic in pre-and post-buckling regimes. The study applies the finite element model (FEM) that considers the effect of both material and geometric nonlinearities. It is concluded that the proposed finite element method accurately predicts the hysteresis curves under cyclic lateral loading and the load-deflection curve under pushover lateral loading in the presence of constant axial loading. Therefore, the adopted finite element method can be confidently used to analyze prismatic thin-walled circular steel tubular columns under pushover and cyclic lateral loading. Also, it is concluded that the envelope curves from hysteresis behavior closely match the load-deflection curves under pushover loading. Therefore, pushover analysis provides lateral load-deformation responses that can evaluate such structures' cyclic behavior a lower analysis time and cost.

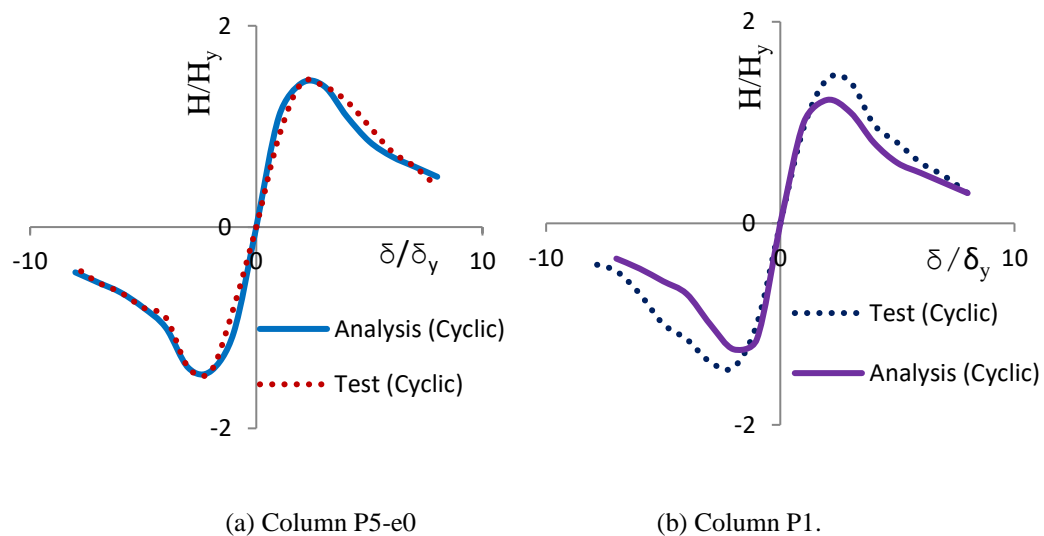


Fig.7: Comparison of envelope curve from tests and analysis.

References

- [1] E. Watanabe, K. Sugiura, K., & W.O. Oyawa, "Effects of multi-directional displacement paths on the cyclic behaviour and seismic design of rectangular hollow steel columns." *Doboku Gakkai Ronbunshu*, 2000(647), pp.79–95. <https://doi.org/10.2208/jscej.2000.647>
- [2] Mamaghani, I. H. P. (1996). *Cyclic Elasto-Plastic Behaviour of Steel Structures: Theory and Experiment*. [PhD dissertation]. University of Nagoya, Nagoya, Japan.
- [3] Esper, P., & Tachibana, E. (1996). Lessons Learned from Kobe Earthquake. *Geological Journal*. Fukumoto, Y., Uenoya, M., & Nakamura, M. (2003). Cyclic performance of stiffened square box columns with thickness tapered plates. *Steel Structures*, 3, 107–115.
- [4] Mamaghani, I. H. P. (2008). Seismic Design and Ductility Evaluation of Thin-Walled Steel Bridge Piers of Box Sections. *Transportation Research Record: Journal of the Transportation Research Board*, 2050(1), pp. 137–142. <https://doi.org/10.3141/2050-14>
- [5] Q. Al-Kaseasbeh, I. H. P. Mamaghani "Performance of Thin-Walled Steel Tubular Circular Columns with Graded Thickness under Bidirectional Cyclic Loading". *Structures Congress 2019*, pp.1–10. <https://doi.org/10.1061/9780784482230.001>

- [6] Q. Al-Kaseasbeh, I. H. P. Mamaghani, "Buckling strength and ductility evaluation of thin-walled steel stiffened square box columns with uniform and graded thickness under cyclic loading". *Engineering Structures*, 186, pp. 498–507, 2019. <https://doi.org/10.1016/j.engstruct.2019.02.026>
- [7] Q. Al-Kaseasbeh, I. H. P. Mamaghani, "Thin-Walled Steel Tubular Circular Columns with Uniform and Graded Thickness under Bidirectional Cyclic Loading". *Thin-Walled Structures*, 145, 106449. <https://doi.org/10.1016/j.tws.2019>
- [8] F. Lyu, Y. Goto, N. Kawanishi, & Y. Xu, "Three-Dimensional Numerical Model for Seismic Analysis of Bridge Systems with Multiple Thin-Walled Partially Concrete-Filled Steel Tubular Columns," *Journal of Structural Engineering*, 146(1), [https://doi.org/10.1061/\(ASCE\)ST.1943-541X.0002451](https://doi.org/10.1061/(ASCE)ST.1943-541X.0002451)
- [9] I.H.P. Mamaghani, M. Khavanin, E. Erdogan & L. Falken, "Elastoplastic Analysis and Ductility Evaluation of Steel Tubular Columns Subjected to Cyclic Loading," *Structures Congress 2008*, pp.1–12. [https://doi.org/10.1061/41016\(314\)298](https://doi.org/10.1061/41016(314)298)
- [10] I.H.P. Mamaghani, & J. A. Packer, "Inelastic behavior of partially concrete-filled steel hollow sections," *4th Structural Specialty Conference of the Canadian Society for Civil Engineering*, Montréal, Québec, Canada, s71, 2002, pp.1–9.
- [11] I.H.P. Mamaghani, T. Usami, & E.Mizuno, "Hysteretic behavior of compact steel box beam-columns", *Journal of Structural Engineering*, 43, pp.187–194, 1997.
- [12] T. Aoki, T., & K. A. S. Susantha, "Seismic Performance of Rectangular-Shaped Steel Piers under Cyclic Loading", *Journal of Structural Engineering*, 131(2), pp. 240–249, 2005. [https://doi.org/10.1061/\(ASCE\)0733-9445\(2005\)131:2\(240\)](https://doi.org/10.1061/(ASCE)0733-9445(2005)131:2(240))
- [13] S. Gao, T. Usami, & H. Ge, "Eccentrically Loaded Steel Columns under Cyclic In-Plane Loading", *Journal of Structural Engineering*, 126(8), pp. 964–973, 2000. [https://doi.org/10.1061/\(ASCE\)0733-9445\(2000\)126:8\(964\)](https://doi.org/10.1061/(ASCE)0733-9445(2000)126:8(964))
- [14] H. Ge, S. Gao, & T. Usami, "Stiffened steel box columns. Part I: Cyclic behavior". *Journal of Engineering Structures*, 29, pp.1691–1706, 2000.
- [15] Y. Goto, Y., T. Ebisawa, & X. Lu, "Local Buckling Restraining Behavior of Thin-Walled Circular CFT Columns under Seismic Loads", *Journal of Structural Engineering*, 140(5), 04013105, 2014. [https://doi.org/10.1061/\(ASCE\)ST.1943-541X.0000904](https://doi.org/10.1061/(ASCE)ST.1943-541X.0000904)
- [16] Y. Goto, Q. Wang, & M. Obata, "FEM Analysis for Hysteretic Behavior of Thin-Walled Columns", *Journal of Structural Engineering*, 124(11), pp. 1290–1301, 1998. [https://doi.org/10.1061/\(ASCE\)0733-9445\(1998\)124:11\(1290\)](https://doi.org/10.1061/(ASCE)0733-9445(1998)124:11(1290))
- [17] K. Nishikawa, S. Yamamoto, T. Natori, K. Terao, H. Yasunami, & M. Terada, "Retrofitting for seismic upgrading of steel bridge columns". *Engineering Structures*, 20(4–6), pp. 540–551, 1998. [https://doi.org/10.1016/S0141-0296\(97\)00025-4](https://doi.org/10.1016/S0141-0296(97)00025-4).
- [18] Y.B. Kwon, N.G. Kim, & G.J. Hancock, "Compression tests of welded section columns undergoing buckling interaction". *Journal of Constructional Steel Research*, 63(12), pp. 1590–1602, 2007. <https://doi.org/10.1016/j.jcsr.2007.01.011>
- [19] H. Li, X. Gao, Y. Liu, & Y. Luo, "Seismic performance of new-type box steel bridge piers with embedded energy-dissipating shell plates under tri-directional seismic coupling action". *International Journal of Steel Structures*, 17(1), pp.105–125, 2017. <https://doi.org/10.1007/s13296-015-0192-z>
- [20] S.A.A. Mustafa, O. M. Elhussieny, E.B. Matar & A.G. Alaaser, "Experimental and FE analysis of stiffened steel I-column with slender sections. *Ain Shams Engineering Journal*, 9(4), pp. 1635–1645, 2018. <https://doi.org/10.1016/j.asej.2016.12.00>
- [21] D.N. Serras, K.A. Skalomenos, G.D. Hatzigeorgiou, & D.E. Beskos, "Modeling of circular concrete-filled steel tubes subjected to cyclic lateral loading". *Structures*, 8, pp. 75–93, 2016. <https://doi.org/10.1016/j.istruc.2016.08.008>
- [22] A. Ucak, & P. Tsopelas, "Accurate modeling of the cyclic response of structural components constructed of steel with yield plateau". *Engineering Structures*, 35, pp.272–280, 2012. <https://doi.org/10.1016/j.engstruct.2011.10.015>
- [23] Z.M. Dalia, A.K. Bhowmick, & G.Y. Grondin, "Local buckling of multi-sided steel tube sections under axial compression and bending". *Journal of Constructional Steel Research*, 186, 106909, 2021. <https://doi.org/10.1016/j.jcsr.2021.106909>
- [24] Q. Al-Kaseasbeh, and I.H.P. Mamaghani, I. H. P., "Thin-Walled Steel Stiffened Square Box Columns with Uniform and Graded Thickness under Bidirectional Cyclic Loading", *Journal, Engineering Structures*, Volume 219, 1 June 2020, <https://reader.elsevier.com/reader/sd/pii/S0141029619318061?token=D0C108ABF1191FD70152E99DF761CF34207600C67A1B3BBDBA46972A07B6A621EE31C93B812AEAEFA3371231AC7BE249>
- [25] Hibbit, K., & Sorensen. (2014). *Abaqus 2014 Documentation; 2014*.